The Journal of Experimental Biology 211, 2576-2583
Published by The Company of Biologists 2008
doi:10.1242/jeb.020164

Micromechanical properties of consecutive layers in specialized insect cuticle: the gula of *Pachnoda marginata* (Coleoptera, Scarabaeidae) and the infrared sensilla of *Melanophila acuminata* (Coleoptera, Buprestidae)

Martin Müller[1], Maciej Olek[2], Michael Giersig[2] and Helmut Schmitz[1,*]

[1]Institute for Zoology, University of Bonn, Poppelsdorfer Schloss, D-53115 Bonn, Germany and [2]Forschungszentrum caesar, Ludwig-Erhardt-Allee 2, D-53175 Bonn, Germany

*Author for correspondence (h.schmitz@uni-bonn.de)

Accepted 10 June 2008

SUMMARY

Insect cuticle is a highly adaptive material that fulfils a wide spectrum of different functions. Cuticle does not only build the exoskeleton with diverse moveable parts but is also an important component of a stunning variety of mechanosensory receptors. Therefore, the mechanical properties of these specialized cuticular systems are of crucial importance. We studied the different cuticular layers of the head part (gula) of the head-to-neck ball articulation of *Pachnoda marginata* and of the photomechanic infrared (IR) sensilla of *Melanophila acuminata* on the basis of cross sections. In our study, we combined histological methods (i.e. detection of the different types of cuticle by specific staining) with measurements of hardness (H) and reduced elastic modulus (E_r) by nanoindentation technique. In the gula of *Pachnoda* we found an unusual aberrance from the well-known layering. Between the epi- and exocuticle, two meso- and one endocuticular layers are deposited which are softer and more elastic than the underlying exo- and mesocuticular layers. The hardest of all examined materials is the cuticle of the exocuticular shell of the internal sphere of the *Melanophila* IR sensillum with H=0.53 GPa whereas the inner mesocuticular core of the sensillum represents the most elastic and softest layer with values of H=0.29 GPa and E_r=4.8 GPa. Results are discussed with regard to the proposed functions.

Key words: insect cuticle, mechanical property, articulation, nanoindentation, atomic force microscopy, infrared receptor.

INTRODUCTION

Insect cuticle fulfils a great variety of functions (Gorb, 2001; Neville, 1975). In addition to its main function, i.e. building the exoskeleton and protecting the inner organs, cuticle is an important component of insect sensilla.

In the exoskeleton, the mechanical properties of joints are of special interest because articulations have to fulfil numerous tasks. For instance, both components of the head articulation system of *Pachnoda marginata* (i.e. the gula part of the ventral head and its counter surface of the prothorax) are in permanent contact with each other and, therefore, must be resistant to wear and friction. Simultaneously, gliding has to function with as little obstruction as possible. Recently, the mechanical properties (hardness and reduced elastic modulus) of the superficial cuticle layers of the gula have been measured by nanoindentation (Barbakadze et al., 2006). Interestingly, the existence of softer and more compliant layers in the exocuticle could be shown. To further investigate this phenomenon, we made cross sections through the gula cuticle and determined the mechanical properties of the different layers on a microscale. For the identification of the different types of cuticle we stained the sections with Mallory trichrome stain.

Furthermore, the structure and composition of the external cuticular apparatus of a sensillum determines which kind of stimulus is perceived (Altner and Loftus, 1985; Steinbrecht, 1984; Thurm, 1969). Thus, the modality of a given sensillum can be deduced from the construction of its cuticular components, which serve for stimulus transmission (Keil, 1997). Additionally, the cuticular apparatus often filters and amplifies a stimulus. This is especially true for cuticular mechanoreceptors, where the mechanical properties of the different types of cuticle determine the specific function (i.e. perception of touch, wind speed, airborne sound, gravity, etc.) and the sensitivity of the receptor (Barth, 1999; French et al., 2002; Hossl et al., 2007; Humphrey and Barth, 2008).

About 70 spherical infrared (IR) sensilla of pyrophilous *Melanophila* beetles (Coleoptera, Buprestidae) are housed in special (IR) pit organs located on both sides of the metathorax (Evans, 1966; Vondran et al., 1995). Recently, it has been shown that the IR sensilla have evolved from cuticular hair mechanoreceptors. Based on the mechanosensitive heritage of the IR sensilla, Schmitz and coworkers have established a refined functional model of the transduction mechanism (Schmitz et al., 2007). IR radiation causes a brief increase in pressure inside the spherical sensillum, which is measured by a mechanoreceptor [the so-called photomechanic mechanism of IR perception; cf. Fig. 6A (Schmitz and Bleckmann, 1998)]. Because the cuticular apparatus accomplishes the conversion of IR radiation into a micromechanical event, the determination of the thermo-mechanical properties of the different components is of particular interest. In a first approach, we measured hardness and modulus of different areas of individual sensilla. Mechanical properties such as elastic modulus and hardness of a given material are mainly determined by the bond strengths (i.e. the interatomic forces within the material). In addition, strong interatomic forces are associated with low thermal expansion, while weak forces are associated with high expansion (Newnham, 2005). Therefore, the information about elastic modulus and hardness can provide valuable insight in the thermal expansion behaviour of a material. A manifestation of this correlation can be observed for example in polymers where an increase of cross-linking leads to an increase in hardness and stiffness and to a decrease of thermal expansion (Nielsen, 1969).

As in the case of the gula cuticle, we used cross sections through individual IR sensilla to measure the mechanical properties of the different cuticular layers. For the identification of the different types of cuticle, the Mallory trichrome stain protocol was used. The gula of *Pachnoda* and the IR sensillum of *Melanophila* are highly specialized cuticular systems. In a comparative approach, we wanted to demonstrate how special structures having fundamentally different functions can be created on the basis of common endo-, meso- and exocuticle. However, the mechanical properties of the different cuticular layers play a key role for the function in both systems. By applying our methods to both systems, we could not only compare the different systems but also relate our results to previous work. Thus, our study is the first attempt to determine mechanical properties of defined microstructured layers of insect cuticle. Results are discussed with respect to the function of specialized cuticles in joints and IR sensing.

MATERIALS AND METHODS

Animals

Burnt logs infested with larvae of *Melanophila acuminata* DeGeer were collected on burnt areas in Catalonia (Spain) in March 2006. The forest fire occurred in summer 2005. The wood was stored in the animal house of the Zoological Institute of Bonn University, where beetles hatched from the wood during the summer months of 2006 and 2007. Beetles were kept in small containers and fed with raisins, peanuts and walnuts. Water was given *ad libitum*. *Pachnoda marginata* Drury beetles were supplied from the Aquazoo Löbbecke Museum (Düsseldorf, Germany).

Sample preparation

Infrared organs were excised from the metathoracic segments of *M. acuminata* beetles and stored either in 30% ethanol [for subsequent embedding in water-soluble Durcupan® (Fluka, Buchs, St Gallen, Switzerland)] or in 70% ethanol [for embedding in Epon 812 (Roth, Karlsruhe, Germany)]. Gula plates were excised from the median ventral plates of heads of *P. marginata* and processed in the same way. Some gula plates were air dried and mounted onto holders by epoxy glue.

Specimens scheduled for embedment in Durcupan® were dehydrated through a series of Durcupan A and water, with an increasing Durcupan A fraction, and finally embedded in a mixture of Durcupan A, hardener, accelerator and plasticizer (Kushida, 1964; Stäubli, 1960). A second set of specimens was dehydrated through an ascending ethanol series and embedded in Epon 812 (Luft, 1961). Samples were cured at 60°C for 3 days.

At this point it should be emphasized that fixation and especially dehydration most probably have changed the material properties of the biological samples. In the Discussion, an attempt will be made to infer the mechanical properties of the native cuticular material as well as using data from the literature where hydrated cuticle (e.g. the gula of *Pachnoda*) had been examined.

Semi-thin sections (0.5 μm thick) from the respective specimen were cut with a Reichert OMU3 microtome (Wien, Austria) using a diamond knife (DiATOME Histo, Biel, Switzerland). Sections were stained with a 0.05% Toluidine-Blue/borax solution and examined with a Leitz DM RBE light microscope (Leica, Wetzlar, Germany). As soon as a suitable cross-sectional profile was reached, the surface was polished by decreasing the slicing thickness down to ~150 nm. In the measurements with the atomic force microscope (AFM) and the nanoindenter, these smoothed surfaces of the epoxy block were probed.

Staining of semi-thin sections with Mallory trichrome stain

Some of the sections were specifically stained to reveal the different types of cuticle. Prior to the staining procedure, the Epon resin was removed by immersion in alcoholic KOH solution (Weyda, 1982). Chemical treatment of the sections with potassium dichromate, acid fuchsin and phosphotungstic acid hydrate was followed by a final staining process for 7 min with a Mallory trichrome solution (Weyda, 1982). Non-melanized exocuticle, which does not really stain, appears in a faint yellow or amber whereas mesocuticle appears red and endocuticle appears blue (Weyda, 1982). Digital images of the sections were taken with a Nikon Coolpix 5000 (Tokyo, Japan).

Atomic force microscopy

To verify the nanoscale topography the samples were examined using an atomic force microscope (FRT MicroProf equipped with a SiS ULTRAObjective® AFM; Bergisch Gladbach, Germany) in non-contact mode with standard tips (Nanosensors PPP-NCLR; Nanosensors, Neuchâtel, Switzerland). Additionally, after the nanoindentation tests, AFM was used to visualise the indents in order to determine the plastic/elastic behaviour of the tested samples.

Nanoindentation

Nanoindentation offers the measurement of hardness and elastic modulus of very small volumes of material (Bhushan and Li, 2003; Oliver and Pharr, 1992). For nanomechanical tests, an AFM (NanoScope IV; Digital Instruments, Santa Barbara, CA, USA) with a conjugated nanomechanical test instrument (TriboScope Hysitron Inc., Minneapolis, MN, USA) was used. The Hysitron nanoindenter is a depth-sensing and load-control device, which is capable of providing measurements of elastic and plastic properties at the nanoscale level. Because it can act like a scanning probe microscope, it allows topography imaging and precise positioning of the tip. In the present study, a Berkovich tip was employed as an indenter. The total included angle of the tip is 142.3°, with a half angle of 65.35°, which makes it very flat and efficient for a wide range of materials, including polymers and biomaterials. The hardness (H) and reduced elastic modulus (E_r) were evaluated by the nanoindenter software from the recorded unloading step of the depth-displacement curve, based on the method of Oliver and Pharr (Oliver and Pharr, 1992). H can be described by the term:

$$H = \frac{F_{max}}{A}\ , \tag{1}$$

where F_{max} is the maximal applied loading force, and A is the contact area. The contact stiffness (S) is defined as the slope of the upper portion of the unloading curve and was calculated by fitting the initial portion of the unloading curve (typically 20–90% of F_{max}) by a simple power law relationship:

$$F = \alpha(h - h_f)^m\ , \tag{2}$$

where the indentation depth (h) and the loading force (F) are the variables and α, m and h_f are determined by the fitting procedure. In this function, h_f equals the final indentation depth, i.e. the depth where the loading force is completely removed (F=0). Finally, the slope at the maximum indentation depth (h_{max}) can be derived. By means of the contact stiffness, E_r can be calculated by the formula:

$$E_r = \frac{\sqrt{\pi}}{2}\frac{S}{\sqrt{A}} \tag{3}$$

and, as can be seen, is also a function of the contact area. Since the contact area is a function of the contact depth, a tip calibration

procedure was employed to determine the geometry of the indenter tip. For this purpose, a series of indentations at different contact depths was carried out on fused quartz; a standard material with well-known properties [elastic modulus (E)=69.6 GPa, H=9.5 GPa] (Oliver and Pharr, 1992). In a calibration process, the projected contact area could be evaluated and used to calculate the E_r and H of the cuticular material. Furthermore, E can be determined by the relationship:

$$\frac{1}{E_r} = \frac{1-\nu^2}{E} + \frac{1-\nu_i^2}{E_i}, \quad (4)$$

where ν is the Poisson's ratio, and E_i and ν_i are the material properties of the Berkovich indenter. Since we used a diamond tip with a high elastic modulus (E_i=1170 GPa) and a low Poisson's ratio (ν_i=0.07), the right-hand term is negligible and the formula can be reduced to:

$$E = E_r(1-\nu^2) . \quad (5)$$

Unfortunately the Poisson's ratio of insect cuticle has not been described satisfactorily yet. Thus, we describe stiffness and elastic modulus by means of E_r.

The epoxy blocks containing the IR organ samples were glued to silicon discs and fixed on the AFM probe-stage using a vacuum system. In a typical nanoindentation experiment, a trapezoidal loading pattern with a maximum load of 300 μN and a load/unload rate of 30 μN s^{-1} (Fig. 1A) was applied. To minimize the effect of material creep, a hold time of 10 s was set after maximum load was reached and before unloading (Chudoba and Richter, 2001). More than 260 indents were performed on 16 sensilla from four IR organs originating from three *Melanophila* beetles. Indents were made in the mesocuticle of the sphere, in the region of the lamellated shell, in the adjacent mesocuticle and also in resin. Furthermore, we measured material properties of the outer surface of one air-dried gula with 20 indents and across all layers of cross-sectioned gula cuticle of one *Pachnoda* beetle with 198 indents. The tips were cleaned with ethanol after several cycles of indentation.

Statistical analysis

The experimental data from nanoindentation measurements were grouped into material classes according to the particular experiments performed on the specific parts of the samples and in relation to the different cuticle compositions that were determined by the Mallory staining. H and E_r of each class were averaged, and the standard deviations (s.d.) were calculated. The results are discussed with respect to the direct comparison of the mean values (H and E_r) of particular material classes by means of a one-way analysis of variance (ANOVA) test. The significance level was set at P<0.05.

RESULTS

Comparison of the cuticular composition of the *Melanophila* IR organ and of the gula region of *Pachnoda*

Mallory trichrome staining revealed that the cuticle of the IR organ of *Melanophila* mainly consists of exo- and mesocuticle (Fig. 2A). The hemispherical bulge that covers the inner sphere comprises an outer layer of unpigmented exocuticle followed by a thin layer of mesocuticle. Most probably because it is too thin, an outermost layer of epicuticle cannot be discerned in the semi-thin sections. The inner sphere is made of an outer exocuticular shell that encloses a mesocuticular core. The sharp boundary between these two components of the sphere can also be seen in the AFM image (Fig. 2B). Also visible in the AFM image is the lamellated

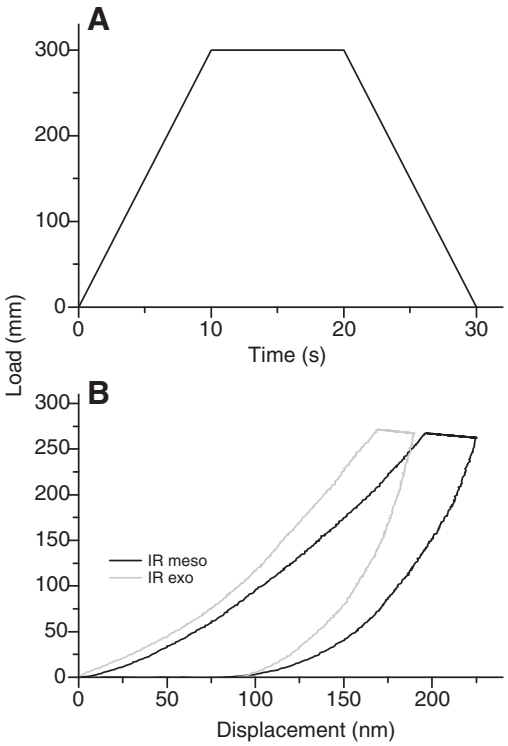

Fig. 1. (A) Applied trapezoidal loading pattern with holding time of 10 s (plateau of curve) to reduce influence of material creep. (B) Representative load–displacement curves for the exocuticular outer shell (IR exo) and the inner mesocuticular core (IR meso) of the *Melanophila* sensillum.

composition of the mantle, which is caused by the layered arrangement of chitin fibres. The sample preparation process does not guarantee a central cross-sectional cut through the sensilla examined, and therefore the previously described small, pear-shaped exocuticular core inside the sphere (Schmitz et al., 2007; Schmitz and Bleckmann, 1997; Vondran et al., 1995) could not be identified in AFM images. The mesocuticle continues to the inner surface of the cuticle of the whole organ. Only small islets of presumed endocuticle could be identified in the more basal layers of the cuticle (Fig. 2A).

In contrast to the IR organ of *Melanophila*, the cuticle of the gula of *Pachnoda* reveals a well-developed layer of inner endocuticle (cf. Barbakadze et al., 2006), which is reduced to a very thin layer of 5 μm or less at the caudal end of the gula (Fig. 3B). Furthermore, a second layer of endocuticle can be found near the outer surface (Fig. 3A,C). The arrangement of the different layers of cuticle is unusual in this area of the gula: between the thin outer epicuticle and the exocuticle, two layers of mesocuticle are situated, with a thin layer of endocuticle in between (Fig. 3A–C). These layers are not as smooth as the other layers of the *Pachnoda* gula, as can be seen in the AFM topography (Fig. 3D,E). Thus, the granular topography may indicate a micro/nanostructured material. For clear identification, we named the layers of the gula cuticle on the basis of their staining results and numbered equally stained layers serially, ascending from the outer to the inner surface of the cuticle.

Mechanical properties

Typical load–displacement curves obtained for the cuticle of the *Melanophila* sensillum are shown in Fig. 1B. At the same indentation load, a higher displacement was achieved for the mesocuticular core of the sphere than for the exocuticular shell. The maximum load of

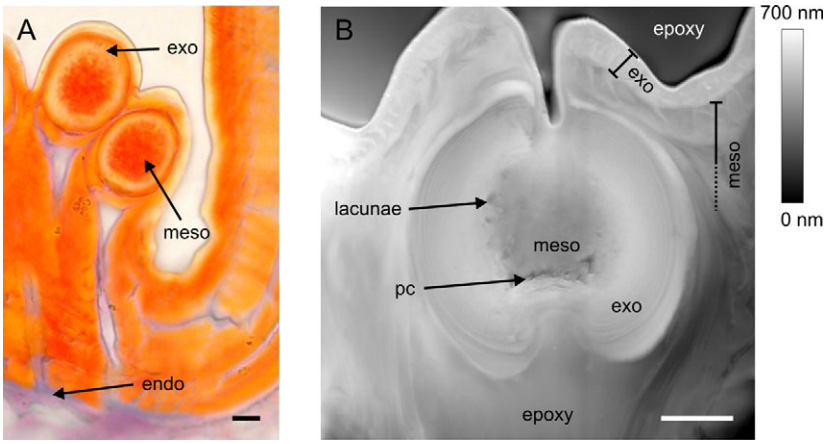

Fig. 2. Cuticle structure of the infrared organ of *Melanophila*. (A) Light microscopical image of two eccentrically cut sensilla stained with Mallory trichrome stain. Yellowish colour indicates unpigmented (β-sclerotized) exocuticle (exo), red indicates mesocuticle (meso), blue indicates endocuticle (endo). (B) AFM topography of one centrally cut sensillum. The layered exocuticular shell surrounds an inner spongy mesocuticle with lacunae and a pressure chamber (pc). Scale bars, 5 μm.

300 μN resulted in contact depths in the range of 120–400 nm (depending on the tested material) and indentation diameters of approximately 0.5–2 μm.

Hardness (H) and reduced elastic modulus (E_r) of the embedding resins used in our study (Durcupan and Epon) were significantly lower than corresponding values of H and E_r of all kinds of examined cuticle (Fig. 4, Table 1). Thus, during probing, the resin could be clearly distinguished from other materials and, therefore, was used as a reference material.

Hardness of the exocuticular shell of the *Melanophila* sensillum was 0.53±0.25 GPa, which is significantly harder than all other types of tested cuticle (Fig. 4, Table 1). Hardness of the exocuticular shell was almost twice that of the mesocuticular core of the sphere (0.29±0.1 GPa), which is the softest of all tested embedded biomaterials.

Hardness of the mesocuticular core of the *Melanophila* sensillum was clearly lower than that of the mesocuticle below the spheres (0.34±0.09 GPa) but differed only insignificantly from the hardness of the outer endocuticular layer and the mesocuticular layer 2 of the *Pachnoda* gula. However, hardness of the inner mesocuticular layer 3 of the gula was significantly higher than hardness of both kinds of mesocuticle identified in the *Melanophila* IR organ and

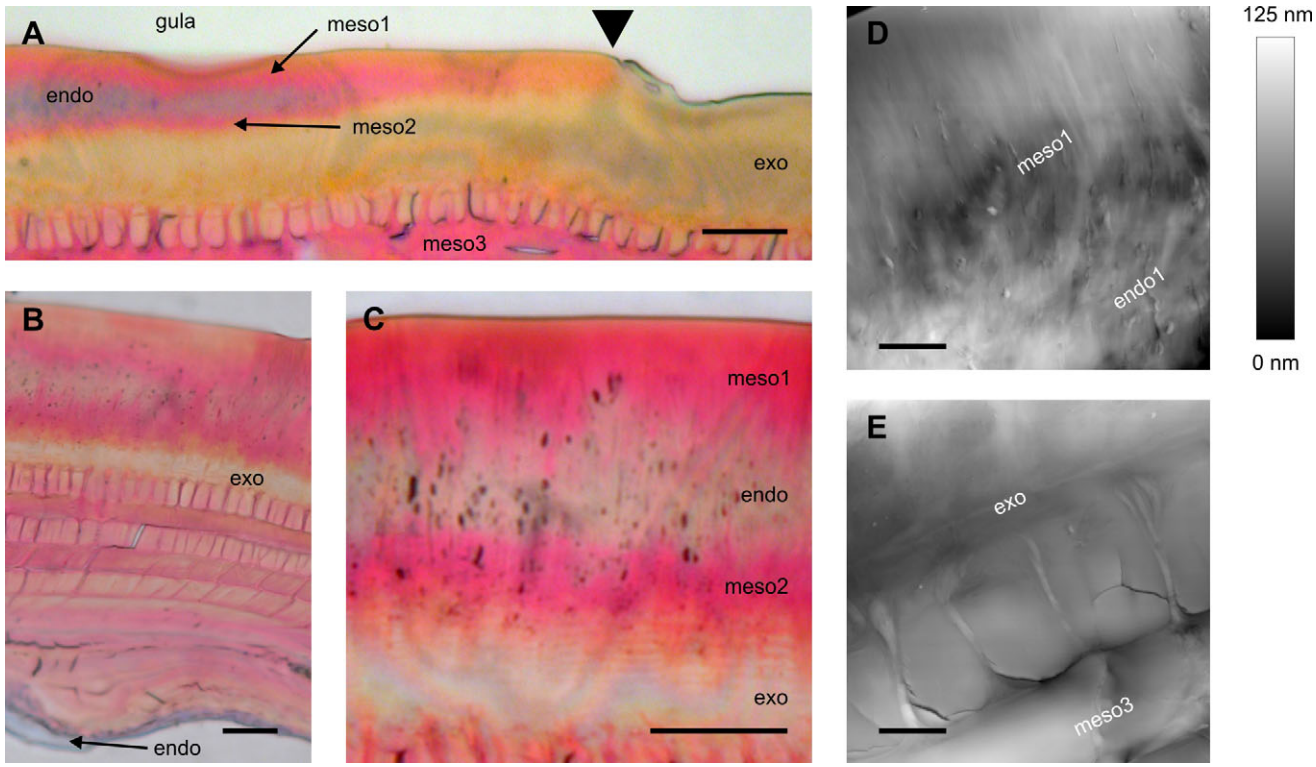

Fig. 3. Cuticle structure of the gula of *Pachnoda marginata*. (A–C) Light microscopical images of Mallory trichrome stained gula sections. Scale bars, 20 μm. (D–E) Topography images made with an atomic force microscope. Scale bars, 5 μm. (A) Rostral beginning of the gula plate (from arrowhead to the left). The unusual layering of the cuticle starts to develop in the centre of the image and extends to the left. Yellowish-stained exocuticle (exo) is superimposed by red-stained mesocuticle (meso) and blue-stained endocuticle (endo). (B) Image of the region probed with the nanoindenter. Only a very thin layer of endocuticle can be distinguished. (C) Magnification of the unusual surface region. (D) Topography of the sliced outer meso-/endocuticular layers, which appear grainy and differ from the smooth cut exocuticle and mesocuticle 3 (meso3) layers shown in E.

also significantly higher than the two outer mesocuticular layers 1 and 2 of the gula.

The hardest layers of *Pachnoda* were the exocuticular layer, where hardness was 0.40±0.07 GPa, and the inner mesocuticular layer 3 (0.43±0.08 GPa). The slight difference between these layers was not significant, but they differed clearly from all other tested materials. Thus, the inner mesocuticular layer 3 showed about the same hardness as the exocuticle of the gula.

In contrast to the *Melanophila* IR organ, endocuticle could be detected in two areas in the cuticle of the gula of *Pachnoda* (Fig. 3B), but the inner layer was not probed, since we placed the nanoindenter tip at the region where the inner endocuticle is reduced. Hardness of the thin outer endocuticular layer was 0.3±0.05 GPa, which only differed slightly from the hardness of the mesocuticular layer 2 of the gula and both kinds of mesocuticle of the *Melanophila* IR organ and, therefore, is the softest layer of the gula of *Pachnoda*.

Hardness of the entire cuticle of the *Pachnoda* gula determined from outside was 0.21±0.03 GPa. This value is significantly lower than *H* of all embedded types of cuticle.

The corresponding elastic modulus differences between particular material classes are somehow dissimilar to the respective hardness data (Fig. 4, Table 1). Our elastic modulus results also reveal the significant differences between the structural sections of the cuticles examined. For example, the highest measured E_r of 9.9±3.0 GPa refers to the inner mesocuticular layer 3 of the gula. By contrast, Young's moduli of the exocuticle of the gula and the exocuticle of the outer shell of the sphere of the *Melanophila* IR sensillum are statistically comparable (8.4±3.4 GPa and 7.9±2.8 GPa, respectively). The modulus of the exocuticle of the *Melanophila* sensillum also did not differ statistically from the modulus of the mesocuticle below the spheres of the IR organ (6.8±1.9 GPa). However, the mesocuticle below the spheres of the IR organ is significantly stiffer than mesocuticle 1 and 2 and also the outer endocuticular layer of the gula. The most elastic material is the mesocuticle inside the sphere of the *Melanophila* sensillum (4.8±1.4 GPa). The modulus of this kind of cuticle is significantly lower than the moduli of all other kinds of examined cuticle except for mesocuticular layer 2 of the gula of *Pachnoda*, which had a modulus of 5.5±0.6 GPa and differed only slightly.

Experiments on the outer surface of the gula revealed a modulus of 6.2±1.3 GPa. Stiffness of the three outermost layers of the gula and the mesocuticle below the spheres of the *Melanophila* IR organ does not differ significantly from this value. The modulus of the mesocuticle inside the sphere of the *Melanophila* sensillum is significantly lower, and the modulus of the exocuticular shell of the *Melanophila* sensillum, as well as the three inner layers of the

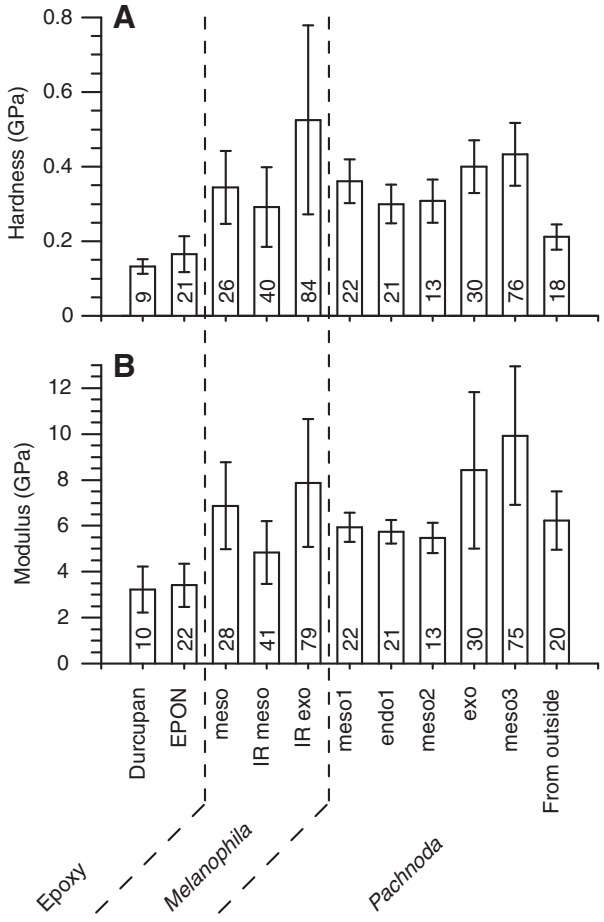

Fig. 4. Means of (A) material hardness and (B) elastic modulus of the different types of cuticle of the *Melanophila* IR organ and the gula plate of *Pachnoda marginata*. Numbers of indents used for calculation are shown inside the bars. Error indicators show standard deviation. Abbreviations: exo, exocuticle; endo, endocuticle; meso, mesocuticle; IR, infrared.

Table 1. ANOVA one-way test for hardness and modulus of the different kinds of cuticles showing significant differences (+) or not (–)

		epoxy		*Melanophila*			*Pachnoda*						
		Durcupan	EPON	meso	IR meso	IR exo	meso1	endo	meso2	exo	meso3	From outside	
Epoxy	Durcupan		–	+	+	+	+	+	+	+	+	+	
	EPON	–		+	+	+	+	+	+	+	+	+	
Melanophila	meso	+	+		+	+	–	–	–	+	+	+	
	IR meso	+	+	+		+	+	–	–	+	+	+	
	IR exo	+	+	–	+		+	+	+	+	+	+	
Pachnoda	meso1	+	+	+	+	+		+	+	+	+	+	Hardness
	endo	+	+	+	+	+	–		–	+	+	+	
	meso2	+	+	+	–	+	+	–		+	+	+	
	exo	+	+	+	+	–	+	+	+		–	+	
	meso3	+	+	+	+	+	+	+	+	+		+	
	From outside	+	+	–	+	+	–	–	–	+	+		
		Modulus											

Significance level was set at $P<0.05$. Upper right corner for significance testing of hardness, lower left corner for modulus.

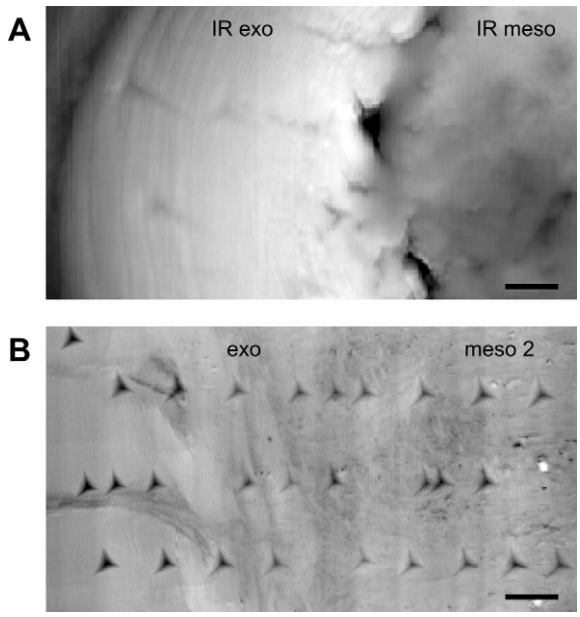

Fig. 5. AFM topography of sections through the *Melanophila* IR sensillum (A) and the *Pachnoda* gula (B) after nanoindentation testing. Some series of residual imprints of the Berkovich tip can be clearly discerned. Imprints on the elastic mesocuticle inside the sphere of the *Melanophila* IR sensillum can hardly be recognized. Scale bars, 1 μm (A); 3 μm (B).

Pachnoda gula, are significantly higher than the modulus of the entire gula cuticle probed from outside.

AFM examination of indents

AFM measurements were performed several days after the indentation experiments so that the materials could recover from the applied strain. Residual imprints were well detected in all *Pachnoda* layers and in the mesocuticle and exocuticular shell of *Melanophila*, but were hardly present in the spongy mesocuticle inside the sphere of the IR sensilla (Fig. 5A,B). This might indicate that deformation recovery is greater in this kind of cuticle. Because of the low indentation depth, residual deformation could not be measured quantitatively.

DISCUSSION

The three-dimensional architecture of the cuticular apparatus of the *Melanophila* IR sensillum demanded the selective opening of the cuticular apparatus in order to investigate the micromechanical properties of the different components. Thus, two-dimensional surface profiles had to be exposed to the tip of the nanoindenter. However, the necessary processing of the cuticle and the probing with the nanoindenter only allowed the investigation of dehydrated material. By contrast, previously published data show to what extent the mechanical properties of the cuticle change if water is removed (Barbakadze et al., 2006; Enders et al., 2004; Hillerton et al., 1982). This allows a well-founded prediction of the condition in the native (i.e. hydrated) phase. Theoretically, some of the embedding resin could have infiltrated the cuticle, thereby changing the mechanical properties. Since sclerotized cuticle is a dense material representing an effective barrier to the environment, intrusion of epoxy chemicals should be impossible but cannot be completely ruled out. Because the embedding resin is much softer than the cuticle, the resulting effects caused by intruding resin should be moderate and restricted to the outer layers. To avoid any further anomalies from the native state we did not apply any chemical fixation. Due to its composition, there is strong evidence that insect cuticle is anisotropic. However, the details of anisotropic behaviour of the cuticles we have investigated are unknown. As in previous studies (Barbakadze et al., 2006; Sachs et al., 2006), we used formulae primarily suitable for the calculation of hardness and modulus of isotropic materials. Because mainly relative differences between the different cuticular layers are of interest in this study we are convinced that this procedure is acceptable.

Recently, the mechanical properties of the gula of *P. marginata* were investigated by nanoindentation (Barbakadze et al., 2006). Hardness and modulus were determined by probing the outer surface of the gula plate. The authors found a sharp drop in hardness values for dry and chemically treated samples at a depth of 1.7 μm. This indicates the presence of softer and more compliant layers in the exocuticle. This interesting finding encouraged us to further investigate this phenomenon. Therefore, we subjected the gula cuticle to the same procedures of embedding and sectioning as the *Melanophila* IR organs.

Functional aspects of the mechanical properties of the gula of *Pachnoda*

Barbakadze and co-workers determined the hardness of the entire dried gula measured from outside as 0.49 GPa and the elastic modulus as 7.5 GPa (Barbakadze et al., 2006). In principle, these data are in the same order of magnitude as our data for hardness (0.21 GPa) and modulus (6.2 GPa) measured from outside. Our somewhat lower values can be explained by a slightly higher water content of our specimens because, unlike their study, we did not dry the cuticle in an oven for 24 h at 40°C. Furthermore, the difference in hardness between the sectioned material of the outer mesocuticular layer (meso 1, H=0.36 GPa) and the gula probed from outside (H=0.21 GPa) could be explained by a change in load direction. A possible explanation may be a pronounced anisotropy of the mesocuticular material. Thus, our data are comparable to the data of Barbakadze et al., which also demonstrates that results obtained at the sectioned cuticle are reasonable too.

Our results show that the cuticle of the gula plate is built with higher complexity than has been described in previous studies (Arzt et al., 2002; Barbakadze et al., 2006; Dai et al., 2006; Enders et al., 2004). The Mallory trichrome stained sections revealed that additional thin layers of meso- and endocuticle overlie the exocuticle (Fig. 3A–C). Fundamental aberrations of the standard cuticular layering have rarely been described (Richards, 1967) and seem to be restricted mainly to larval or pupal stages or to specialized regions in adult insects (e.g. near intersegmental membranes). The histological findings are corroborated by the measurements of the mechanical properties: hardness and modulus of the three outer layers of meso- and endocuticle were significantly lower than the values for the exocuticle (Fig. 4, Table 1). These differences will become even larger in the native phase. Hard cuticle, such as exocuticle, contains only about 12% water whereas softer cuticle can contain 40–70% (Vincent and Wegst, 2004). Mesocuticle is sclerotized to a lesser extent than exocuticle; therefore, the water content is expected to be higher than that of exocuticle and lower than that of endocuticle, which may be due to deposition of different types of proteins in the various layers. Moreover, the water content strongly influences the mechanical material properties, and an increased portion of water makes the cuticle softer and more elastic (Arzt et al., 2002; Barbakadze et al., 2006; Enders et al., 2004; Hillerton et al., 1982; Vincent and Hillerton, 1979; Vincent and Wegst, 2004).

The unusual layering of the gula cuticle can be explained by the specific mechanical requirements of this articulation between the head and the prothorax; when the head is moved relative to the

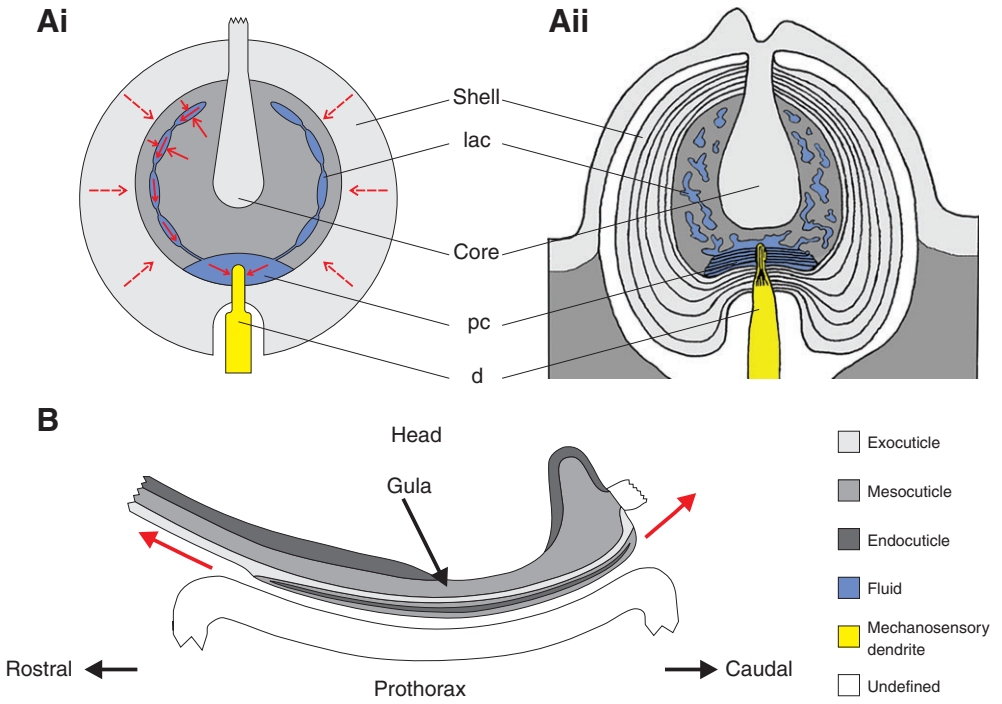

Fig. 6. (A) Structure and proposed function of the *Melanophila* IR sensillum. (i) Schematic demonstrating the functional principle. (ii) A more detailed morphological drawing [adapted from Schmitz et al. (Schmitz et al., 2008)]. Absorption of IR radiation by the cuticle and the fluid causes the mesocuticle and the fluid (blue) inside the lacunae (lac) to expand (indicated by red arrows). This results in an increase in pressure inside the inner pressure chamber (pc), which deforms the tip of the mechanosensory dendrite (d). The hard outer shell functions as a pressure vessel and, as suggested in the Discussion, may even shrink due to slight shortening of the embedded chitin fibres (broken arrows). (B) The structure of the *Pachnoda* gula as a frictional ball joint system. Red arrows indicate a possible direction of head movement.

thorax, the gula glides over the prothoracic counter surface [see red arrows in Fig. 6B, and fig. 2 in Barbakadze et al. (Barbakadze et al., 2006)]. Comparative measurements of dried samples of the head articulation of *Pachnoda* have shown that the head part of this contact pair is harder than the prothoracic counterpart (Arzt et al., 2002), but no histological data to estimate native hydrated material hardness and elastic modulus have been collected. Our results show that the outer surface of the gula does not consist of exocuticle but is covered by a 'pad' consisting of a mesocuticular encasement enclosing a thin layer of endocuticle. Our measurements show that the meso- and endocuticle of the pad are softer and less stiff than the underlying exocuticle. It can be postulated that in the living beetle, where the water content of the mesocuticle and especially the endocuticle is much higher than in dried material, hardness and stiffness will be reduced additionally. Because frictional investigations have suggested that for frictional behaviour the articulation material is one of the most important factors (Dai et al., 2006), we postulate that, in principle, the pad may function as fibrous cartilage. In this type of cartilage, an outer envelope containing fibrous bundles (here the mesocuticular encasement reinforced by chitin fibres) encloses a gelatinous core (the endocuticle). If the pad really does fulfil the function of a layer of cartilage, it provides the articulation with high elasticity and compression strength, which facilitates frictionless movement. Additionally, compressive stress as well as friction and shearing forces are reduced. Fluid components of the epicuticular wax layer could take on the lubricating function of the synovial fluid but this has to be demonstrated. Further investigations have to show to what extent these possible capacities are necessary for the function of the head articulation in *Pachnoda.*

Composition and mechanical properties of the cuticular apparatus of the *Melanophila* IR sensillum: consequences for the possible function

Mallory trichrome staining of the cuticle of the IR organ of *Melanophila* revealed that darkly pigmented outer exocuticle, as well as a distinct layer of inner endocuticle, is missing. The cuticle under the spheres consists of mesocuticle, which also builds the interior thin layer of the dome-shaped bulge covering each sphere. The outer layer of the bulge, however, consists of colourless exocuticle, which is supposed to be β-sclerotized, and is finally covered by a very thin epicuticle (Schmitz et al., 2007). The sphere, in which the tip of the mechanosensory dendrite is situated, consists of an outer shell of β-sclerotized cuticle containing an inner mesocuticular core. In this respect, the results of earlier studies were corroborated (Schmitz et al., 2007; Vondran et al., 1995). However, the hardness and the modulus of the mesocuticle inside the sphere are significantly lower than those of the mesocuticle under the spheres (Fig. 4, Table 1). As we have already outlined in the Introduction, there is a close correlation between mechanical and thermo-mechanical material properties. Thus, harder and stiffer cuticular material most probably has a lower coefficient of thermal expansion than more elastic and softer cuticle. According to our model of photomechanic transduction by a photomechanic IR sensillum this would mean that, in the case of IR absorption by the cuticle of the IR organ, the resulting thermal expansion will not be uniform. In fact, thermal expansion of the mesocuticle of the inner core will be restrained by the harder and stiffer exocuticular shell (Fig. 6A). Taking into account that the microcavities inside the mesocuticular core are filled with a fluid, which also shows a much higher coefficient of thermal expansion, this will result in a distinct increase in internal pressure inside the shell of the sphere. The pressure will be transmitted by the incompressible fluid through the canals of the spongy mesocuticle to the inner pressure chamber, where the mechanosensitive tip of the dendrite is situated. Due to the hydraulic function of the fluid, a cross compression of the dendritic tip will take place (cf. Fig. 6A). This is adequate stimulus for an insect mechanoreceptor.

The exocuticular shell of the sphere, therefore, functions as an outer pressure vessel. To act as an expansion-restraining structure, the shell is reinforced by layers of chitin fibres, giving the shell a highly lamellated appearance (Schmitz et al., 2007; Vondran et al.,

1995). The large standard deviation encountered when we measured hardness may be explained by the variation of the angle between the probing direction and the orientation of the chitin fibres. Additionally, in a few cases, layers of chitin fibres of the shell were most probably approached completely perpendicularly. In these cases, we measured a much higher hardness, with a mean value of 0.67 GPa. Therefore, direction of applied load may play a pivotal role for this kind of highly ordered cuticle, and material characteristics are supposed to be anisotropic. Because chitin fibres are extremely resistant to mechanical stress and strain, we postulate that the main reason for the incrustation of chitin fibres in the shell is to secure a minimal thermal expansion of the shell in case of IR absorption; all displacement caused by thermal expansion should be 'concentrated' onto the membrane of the dendritic tip inside the inner pressure chamber.

To further develop the current model of photomechanic transduction, thereby improving its efficiency, even a decrease in the volume of the sphere is imaginable due to a negative coefficient of thermal expansion of the outer shell. Several long-chain polymers and carbon-containing fibres (e.g. carbon fibres) show a thermal contraction along their chain axis but expand radial to the chain direction (Newnham, 2005). Because the chitin fibres are arranged circumferentially, the outer shell would shrink because of the longitudinal contraction and radial expansion of the chitin fibres (Fig. 6A). The resulting decrease in size of the inner lumen inside the shell would additionally increase the rising pressure inside the fluid-filled mesocuticular core. Admittedly, the case of chitin is different from the examples mentioned because chitin fibres typically consist of a bundle of chitin chains that are linked by hydrogen bonds. However, a similar behaviour might be possible and would enhance IR receptor function. This deserves further investigation.

LIST OF ABBREVIATIONS

A	contact area
AFM	atomic force microscope
E	elastic modulus/Young's modulus
E_i	elastic modulus of the Berkovich tip
E_r	reduced elastic modulus
H	hardness
h	indentation depth
h_f	final indentation depth
h_{max}	maximum indentation depth
IR	infrared
lac	lacunae
P	probability of similarity
F	loading force
F_{max}	maximal applied loading force
S	contact stiffness
ν	Poisson's ratio
ν_i	Poisson's ratio of the Berkovich tip

We thank Horst Bleckmann for providing lab space and for his continuous interest in our work. We are indebted to Wilhelm Barthlott (Nees-Institute, University of Bonn) for the permission to use the AFM and to Anke Schmitz for her help with the staining technique. We also thank Marta Miralles Bouver from GRAF (Cerdanyola del Vallès, Spain) for supplying burnt wood infested with *Melanophila* larvae from forest fire areas in Catalonia. The comments of two anonymous referees helped to improve the manuscript considerably. Supported by a grant of the German Federal Ministry of Education and Research to H.S. (Grant No. 01RIO644A).

REFERENCES

Altner, H. and Loftus, R. (1985). Ultrastructure and function of insect thermo- and hygroreceptors. *Annu. Rev. Entomol.* **30**, 273-295.
Arzt, E., Enders, S. and Gorb, S. (2002). Towards a micromechanical understanding of biological surface devices. *Z. Metallk.* **93**, 345-351.
Barbakadze, N., Enders, S., Gorb, S. and Arzt, E. (2006). Local mechanical properties of the head articulation cuticle in the beetle *Pachnoda marginata* (Coleoptera, Scarabaeidae). *J. Exp. Biol.* **209**, 722-730.
Barth, F. G. (1999). Dynamics of arthropod filiform hairs. V. The response of spider trichobothria to natural stimuli. *Philos. Trans. R. Soc. B, Biol. Sci.* **354**, 183-192.
Bhushan, B. and Li, X. D. (2003). Nanomechanical characterisation of solid surfaces and thin films. *Int. Mater. Rev.* **48**, 125-164.
Chudoba, T. and Richter, F. (2001). Investigation of creep behaviour under load during indentation experiments and its influence on hardness and modulus results. *Surf. Coat. Technol.* **148**, 191-198.
Dai, Z. D., Min, Y. and Gorb, S. N. (2006). Frictional characteristics of the beetle head-joint material. *Wear* **260**, 168-174.
Enders, S., Barbakadse, N., Gorb, S. N. and Arzt, E. (2004). Exploring biological surfaces by nanoindentation. *J. Mater. Res.* **19**, 880-887.
Evans, W. G. (1966). Morphology of the infrared sense organ of *Melanophila acuminata* (Buprestidae: Coleoptera). *Ann. Entomol. Soc. Am.* **59**, 873-877.
French, A. S., Torkkeli, P. H. and Seyfarth, E. A. (2002). From stress and strain to spikes: mechanotransduction in spider slit sensilla. *J. Comp. Physiol. A* **188**, 739-752.
Gorb, S. N. (2001). *Attachment Devices of the Insect Cuticle.* Dordrecht: Kluwer Academic Publishers.
Hillerton, J. E., Reynolds, S. E. and Vincent, J. F. V. (1982). On the indentation hardness of insect cuticle. *J. Exp. Biol.* **96**, 45-52.
Hossl, B., Bohm, H. J., Rammerstorfer, F. G. and Barth, F. G. (2007). Finite element modeling of arachnid slit sensilla. I. The mechanical significance of different slit arrays. *J. Comp. Physiol. A* **193**, 445-459.
Humphrey, J. A. C. and Barth, F. G. (2008). Medium flow-sensing hairs: biomechanics and models. In *Advances in Insect Physiology: Insect Mechanics and Control*, vol. 34 (ed. J. Casas and S. J. Simpson), pp. 1-80. London: Academic Press.
Keil, T. A. (1997). Functional morphology of insect mechanoreceptors. *Microsc. Res. Tech.* **39**, 506-531.
Kushida, H. (1964). Improved methods for embedding with Durcupan. *J. Electron Microsc.* **13**, 139-144.
Luft, J. H. (1961). Improvements in epoxy resin embedding methods. *J. Biophys. Biochem. Cytol.* **9**, 409-414.
Neville, A. C. (1975). *Biology of the Arthropod Cuticle.* Heidelberg: Springer-Verlag.
Newnham, R. E. (2005). *Properties of Materials. Anisotropy, Symmetry, Structure.* New York: Oxford University Press.
Nielsen, L. E. (1969). Cross-linking effect on physical properties of polymers. *J. Macromol. Sci. Revs. Macromol. Chem.* **C3**, 69-103.
Oliver, W. C. and Pharr, G. M. (1992). An improved technique for determining hardness and elastic modulus using load and displacement sensing indentation experiments. *J. Mater. Res.* **7**, 1564-1583.
Richards, A. G. (1967). Sclerotization and the localization of brown and black colors in insects. *Zool. Jahrb. Abt. Anat. Ontogenie Tiere* **84**, 25-62.
Sachs, C., Fabritius, H. and Raabe, D. (2006). Experimental investigation of the elastic-plastic deformation of mineralized lobster cuticle by digital image correlation. *J. Struct. Biol.* **155**, 409-425.
Schmitz, A., Sehrbrock, A. and Schmitz, H. (2007). The analysis of the mechanosensory origin of the infrared sensilla in *Melanophila acuminata* (Coeloptera; Buprestidae) adduces new insight into the transduction mechanism. *Arthropod Struct. Dev.* **36**, 291-303.
Schmitz, A., Gebhardt, M. and Schmitz, H. (2008). Microfluidic photomechanic infrared receptors in a pyrophilous flat bug. *Naturwissenschaften* **95**, 455-460.
Schmitz, H. and Bleckmann, H. (1997). Fine structure and physiology of the infrared receptor of beetles of the genus *Melanophila* (Coleoptera: Buprestidae). *Int. J. Insect Morphol. Embryol.* **26**, 205-215.
Schmitz, H. and Bleckmann, H. (1998). The photomechanic infrared receptor for the detection of forest fires in the buprestid beetle *Melanophila acuminata*. *J. Comp. Physiol. A* **182**, 647-657.
Stäubli, W. (1960). Nouvelle matière d'inclusion hydrosoluble pour la cytologie electronique. *C. R. Acad. Sci.* **250**, 1137-1139.
Steinbrecht, R. A. (1984). Chemo-, hygro-, and thermoreceptors. In *Biology of the Integument, 1 Invertebrates* (ed. J. Bereiter-Hahn, A. G. Matoltsy and K. S. Richards), pp. 523-553. Heidelberg: Springer-Verlag.
Thurm, U. (1969). General organization of sensory receptors. In *Processing of Optical Data by Organisms and by Machines* (ed. W. Reichardt), pp. 44-68. New York: Academic Press.
Vincent, J. F. V. and Hillerton, J. E. (1979). Tanning of insect cuticle - a critical review and a revised mechanism. *J. Insect Physiol.* **25**, 653-658.
Vincent, J. F. V. and Wegst, U. G. K. (2004). Design and mechanical properties of insect cuticle. *Arthropod Struct. Dev.* **33**, 187-199.
Vondran, T., Apel, K. H. and Schmitz, H. (1995). The infrared receptor of *Melanophila acuminata* De Geer (Coleoptera: Buprestidae): ultrastructural study of a unique insect thermoreceptor and its possible descent from a hair mechanoreceptor. *Tissue Cell* **27**, 645-658.
Weyda, F. (1982). Adaptation of Mallory's trichrome stain to insect tissue epoxy sections. *Z. Mikrosk. Anat. Forsch.* **96**, 79-80.